

# Study of minority carrier traps in $p$ -GaN gate HEMT by optical deep level transient spectroscopy

Cite as: Appl. Phys. Lett. **120**, 212105 (2022); <https://doi.org/10.1063/5.0083362>

Submitted: 24 December 2021 • Accepted: 16 May 2022 • Published Online: 25 May 2022

Jiaxiang Chen, Wei Huang, Haolan Qu, et al.

## COLLECTIONS

Paper published as part of the special topic on [Wide- and Ultrawide-Bandgap Electronic Semiconductor Devices](#)



[View Online](#)



[Export Citation](#)



[CrossMark](#)

## Lock-in Amplifiers up to 600 MHz



Zurich  
Instruments



# Study of minority carrier traps in $p$ -GaN gate HEMT by optical deep level transient spectroscopy

Cite as: Appl. Phys. Lett. **120**, 212105 (2022); doi: 10.1063/5.0083362

Submitted: 24 December 2021 · Accepted: 16 May 2022 ·

Published Online: 25 May 2022



View Online



Export Citation



CrossMark

Jiaxiang Chen,<sup>1,2,3</sup> Wei Huang,<sup>4</sup> Haolan Qu,<sup>1,2,3</sup> Yu Zhang,<sup>1,2,3</sup> Jianjun Zhou,<sup>5</sup>  Baile Chen,<sup>1</sup>  and Xinbo Zou<sup>1,6,a)</sup> 

## AFFILIATIONS

<sup>1</sup>School of Information Science and Technology, ShanghaiTech University, Shanghai 201210, China

<sup>2</sup>Shanghai Institute of Microsystem and Information Technology, Chinese Academy of Sciences, Shanghai 200050, China

<sup>3</sup>The School of Microelectronics, University of Chinese Academy of Sciences, Beijing 100049, China

<sup>4</sup>School of Microelectronics, Fudan University, Shanghai 200433, China

<sup>5</sup>Science and Technology on Monolithic Integrated Circuits and Modules Laboratory, Nanjing Electronic Devices Institute, 524 East Zhongshan Road, Nanjing 210016, China

<sup>6</sup>Shanghai Engineering Research Center of Energy Efficient and Custom AI IC, Shanghai 200031, China

**Note:** This paper is part of the APL Special Collection on Wide- and Ultrawide-Bandgap Electronic Semiconductor Devices.

<sup>a)</sup>Author to whom correspondence should be addressed: [zouxb@shanghaitech.edu.cn](mailto:zouxb@shanghaitech.edu.cn)

## ABSTRACT

Properties of minority carrier (electron) traps in Schottky type  $p$ -GaN gate high electron mobility transistors were explicitly investigated by optical deep level transient spectroscopy (ODLTS). By temperature-scanning ODLTS, three electron traps, namely, E1, E2, and E3, were revealed, together with activation energy, capture cross section, and trap concentration. A thermally accelerated electron-releasing process of traps was quantitatively studied by Laplace ODLTS with individual emission time constant disclosed. At 300 K, the emission time constant was determined to be 0.21 and 1.40 s for E2 and E3, respectively, which adjacently existed in the bandgap and held activation energies of over 0.6 eV. As varying the optical injection pulse duration, a three-dimensional mapping of capacitance transient was obtained for each trap, attesting to the electron capture capability of each trap. By varying the reverse bias, the analysis of the ODLTS signal amplitude indicates that all three electron traps are located inside the  $p$ -GaN layer rather than the surface defect related.

Published under an exclusive license by AIP Publishing. <https://doi.org/10.1063/5.0083362>

AlGaIn/GaN heterostructure-based high electron mobility transistors (HEMTs) are promising devices for high-power and high-frequency applications, owing to large electron mobility, superior critical electrical field, and outstanding thermal stability.<sup>1–3</sup> Recently, enhancement-mode HEMTs with a  $p$ -GaN gate are receiving extensive research interest for the reasons of easy gate driving and fail-safe properties, in addition to small gate charge and low on-resistance. GaN power IC implemented by E/D-mode transistors and rectifiers has also been demonstrated recently based on a  $p$ -GaN gate HEMT platform.<sup>4</sup>

There have been some studies on the dynamic degradation of  $p$ -GaN gate HEMTs. Current collapse and threshold voltage instability have been reported upon various gate voltage stressing conditions.<sup>5–8</sup> Positive threshold voltage shift,<sup>9,10</sup> which may destructively impact the device on-resistance and the switching speed, has been observed after on-state gate bias stressing and is often linked to electron-trapping in the  $p$ -GaN layer.<sup>10</sup> In addition, it is also pointed out that the emission

process of trapped electrons also exerts influence on the current collapse of  $p$ -GaN gate HEMTs.<sup>11</sup>

Considering reliability issues of the  $p$ -GaN gate HEMTs, it is demanding to investigate deep-level traps in  $p$ -GaN, which are responsible for dynamic degradations. There have been some reports on the majority carrier (hole) traps in  $p$ -GaN layers by deep level transient spectroscopy (DLTS).<sup>12–14</sup> A hole trap with an activation energy of 0.88 eV has been identified and regarded to be originated from carbon impurities ( $C_N$ ).<sup>12,13</sup> However, few studies have been devoted to minority carrier (electron) trap characteristics in the  $p$ -GaN layer, particularly in a  $p$ -GaN gate HEMT.<sup>15,16</sup> As a matter of fact, minority carrier traps<sup>17,18</sup> may reduce the minority carrier lifetime and electrical conductivity that are crucial to high-speed switching operations.<sup>19</sup>

Optical deep level transient spectroscopy (ODLTS)<sup>20,21</sup> with optical stimulus for carrier generation is regarded as a powerful tool to investigate trap behaviors, particularly minority carrier trap properties. For example, electron and hole traps in  $n$ -GaN grown on different

substrates have been studied using 470 and 355 nm LEDs.<sup>21</sup> Nitrogen-site carbon in the *n*-GaN layer has been linked to a hole trap with the help of sub-bandgap-light irradiation.<sup>22</sup> Existing reports show that it is quite challenging to distinguish adjacent multiple trap levels by conventional temperature-scanning DLTS.<sup>16</sup> In order to precisely examine the broad DLTS signal spectrum and make adjacent trap levels distinguishable, advanced DLTS techniques, such as Laplace DLTS,<sup>23,24</sup> could be adopted with electrical or optical stimulus.

In this work, properties of electron traps in the *p*-GaN layer of a *p*-GaN/AlGaN/GaN HEMT have been explicitly investigated by ODLTS techniques. By temperature-scanning ODLTS, three electron traps, namely, E1, E2, and E3 were revealed. Using high-resolution Laplace ODLTS, an individual trap energy level was well resolved. Moreover, temperature-dependent emission time constants of electron traps were also extracted by Laplace ODLTS. To profile the trap capture process and location in the device, the optical pulse duration and reverse bias were varied to manipulate the carrier trapping and de-trapping process. The investigation of minority carrier traps in the *p*-GaN layer via ODLTS provides supportive evidence for understanding the dynamic degradation in *p*-GaN gate HEMTs and gives impetus to further research on minority carrier traps in wide bandgap semiconductors.

The *p*-GaN HEMT used in this study consists of a 70 nm *p*-GaN layer, a 15 nm Al<sub>0.3</sub>Ga<sub>0.7</sub>N barrier layer, and a thick GaN buffer grown on a Si substrate. To perform the ODLTS study, the epilayer was fabricated into Schottky metal/*p*-GaN/AlGaN/GaN diodes, as shown in Fig. 1(a). The Schottky contact was formed by depositing Ni/Au on the *p*-GaN, while Ti/Al/Ni/Au was deposited on the AlGaN layer, followed by thermal annealing to form Ohmic contacts.

Figure 1(b) shows temperature-dependent *I*-*V* characteristics. When the temperature was increased from 50 to 300 K, the turn-on voltage (using 1 A/cm<sup>2</sup> as the threshold criteria) was decreased from 1.71 to 1.52 V due to augmented thermionic emission of electrons flowing from a two-dimensional electron gas to a Schottky contact.

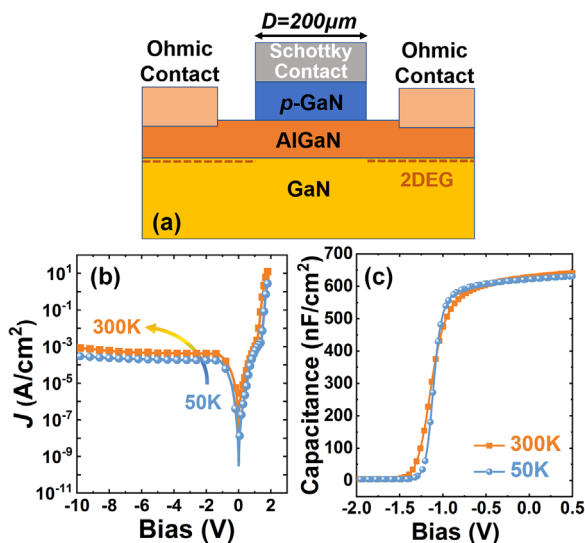


FIG. 1. (a) Schematic of a device structure for ODLTS measurements with a Schottky contact to *p*-type GaN. (b) *I*-*V* curves and (c) *C*-*V* curves.

From 50 to 300 K, the leakage current density is slightly increased from 0.30 to 0.88 mA/cm<sup>2</sup> at -10 V due to enhanced thermal generation of charge carriers in the depletion region. Figure 1(c) plots *C*-*V* characteristics at 50 and 300 K with a measurement frequency of 1 MHz. A relatively sharper transition in capacitance was observed as the temperature decreases. By defining the transition voltage to be the value of the applied voltage, the capacitance variation reached 50% of the total change. The transition voltage was barely shifted from 50 to 300 K due to relatively low Mg doping concentration (in the level of 10<sup>17</sup> cm<sup>-3</sup>) in the *p*-GaN layer.

The temperature-scanning ODLTS spectra were applied to identify the existence and energy levels of traps in the *p*-type GaN layer, as shown in Fig. 2(a). Temperature-scanning ODLTS was conducted using an optical pulse whose duration *t*<sub>po</sub> was set as 100 ms and a reverse bias *U*<sub>R</sub> of -1 V. The optical pulse features a sub-bandgap wavelength of 405 nm, which supplies sufficient energy to activate electrons to be trapped by electron traps in the *p*-GaN layer. From the ODLTS spectrum, the negative ODLTS signals and relatively broad valley observed around 275 K indicated that multiple minority carrier traps existed in the *p*-GaN layer. In total, three electron traps were extracted by the Arrhenius relation

$$\ln(\tau T^2) = \frac{E_C - E_T}{kT} - \ln(\gamma\sigma_n), \quad (1)$$

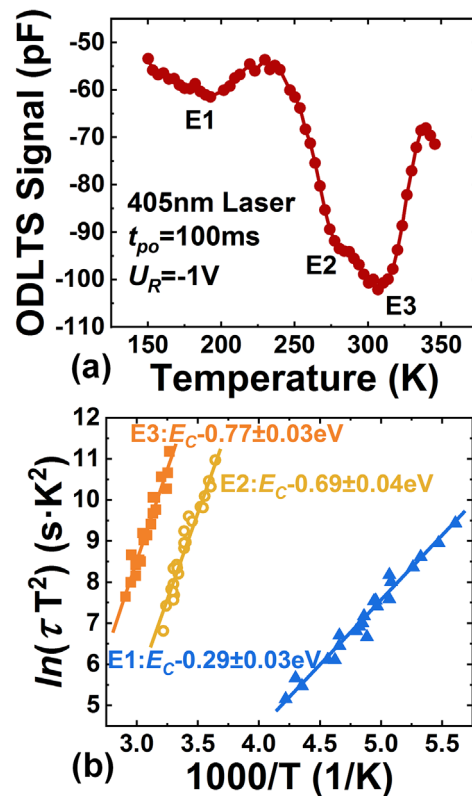


FIG. 2. (a) ODLTS spectrum by temperature-scanning at 1 MHz. (b) Arrhenius plots of three electron traps.

where  $k$  is the Boltzmann constant,  $E_T$  is the energy level of trap states,  $E_C$  is the bottom of the conduction band,  $\sigma_n$  is the capture cross section,  $\tau$  is the emission time constant obtained by ODLTS methods, and  $\gamma$  is a constant related to the effective electron mass.<sup>25</sup>

In addition to electron trap E1 observed around 190 K, two more traps E2 and E3 were extracted from the relative broad valley from 275 to 325 K. Figure 2(b) shows Arrhenius plots of three electron traps obtained from ODLTS spectra. The properties of traps, including the activation energy ( $E_C - E_T$ ), capture cross section ( $\sigma_n$ ), and trap concentration ( $N_T$ ), were summarized in Table I. The trap E1 with the activation energy of  $0.29 \pm 0.03$  eV has the smallest capture cross section and lowest  $N_T$ , showing its relatively weak electron capture capability than the other traps, in good agreement with relatively small ODLTS signal magnitude. E2 ( $E_C - 0.69 \pm 0.04$  eV) and E3 ( $E_C - 0.77 \pm 0.03$  eV) shared similar activation energy, as shown by the overlapping ODLTS signals. Trap E3 has the highest concentration and largest activation energy among all the traps observed, indicating that E3 is the prominent trap level. Given the activation energy of trap E1, deep levels around  $E_C - 0.3$  eV have also been observed in the n-GaN film with high dislocation density,<sup>26</sup> n-GaN on sapphire,<sup>27</sup> and irradiated n-GaN samples.<sup>28</sup> Levels near  $E_C - 0.65$ – $0.75$  eV have been reported elsewhere, e.g., in  $\text{NH}_3$ -molecular beam epitaxy (MBE) and plasma-assisted MBE n-GaN layers, where N-rich growth has been promoted.<sup>29</sup> Levels at  $E_C - 0.7 \pm 0.05$  eV in n-GaN have been reportedly overlapped with some minor levels, forming a broad level in the bandgap.<sup>30</sup> Similar to the activation energy of E3, traps at  $E_C - 0.78$ – $0.81$  eV have been identified in n-GaN layers grown on SiC and Si substrates as well and have been regarded as dislocation-related defects.<sup>21</sup>

Figure 3(a) shows representative Laplace ODLTS<sup>23,24</sup> spectra of trap E1, measured at four different temperatures from 180 to 195 K. In the Laplace ODLTS analysis, the recorded capacitance transients were transformed into spectra by inverse Laplace transformation (ILT) employing Tikhonov regularization<sup>31</sup> (for details see the supplementary material). From 180 to 195 K, only one signal peak could be observed in the Laplace ODLTS spectra. The peak location, which corresponds to the emission time constant, is shifting to the smaller emission time constant side as the temperature is increasing. Figure 3(b) illustrates the temperature-dependent emission time constants ( $\tau_T$ ) of E1 extracted by Laplace ODLTS spectra. As the temperature increases from 170 to 200 K, the  $\tau_T$  of E1 is reduced from 3.50 to 0.23 s, indicating a thermally accelerated electron-releasing process for a filled minority carrier trap. The enhanced thermionic carrier emission agreed well with observations that DLTS peaks of the shallow minority carrier trap in *p*-type GaN occurred at higher temperatures for increased testing frequency.<sup>32</sup> The phenomenon has been reported for hole emission from minority carrier traps of n-GaN with current-injection by the pulsed forward voltage,<sup>22,33</sup> while in this study the

**TABLE I.** Properties of electron traps extracted from temperature-scanning ODLTS.

Trap No.	$E_C - E_T$ (eV)	Capture cross section ( $\text{cm}^2$ )	$N_T \times 10^{15}$ ( $\text{cm}^{-3}$ )
E1	$0.29 \pm 0.03$	$2.94 \times 10^{-17}$	1.08
E2	$0.69 \pm 0.04$	$5.61 \times 10^{-14}$	1.65
E3	$0.77 \pm 0.03$	$2.57 \times 10^{-13}$	1.73

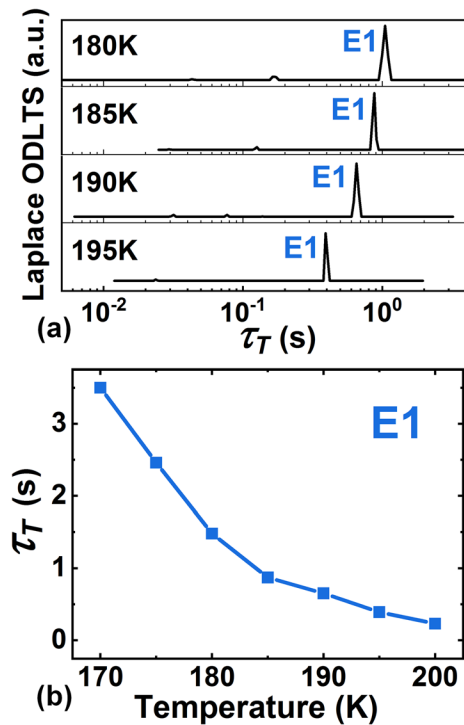


**FIG. 3.** (a) Representative Laplace ODLTS spectra of E1 from 180 to 195 K. (b) The temperature-dependent emission time constant ( $\tau_T$ ) of E1 extracted from Laplace ODLTS.

emission time constant was quantitatively extracted for minority carrier traps in the *p*-GaN layer with the help of sub-bandgap optical stimulus. Given the thermal emission time constants, the activation energy of E1 could be extracted around  $E_C - 0.27$  eV in the Arrhenius plot according to Eq. (1). The activation energy was quite consistent with the results of temperature-scanning ODLTS. Trap E1 obtained in this study exhibits a relatively larger capture cross section than a similar electron trap ( $E_C - 0.23$  eV) of a *p*-GaN HEMT, also revealed by DLTS measurements in the literature;<sup>34</sup> however, the value in our sample was limited to be as small as  $2.94 \times 10^{-17} \text{ cm}^2$ , indicating E1 has a weaker capability of capturing electrons.

Figure 4(a) shows a representative capacitance transient at 300 K, in which E2 and E3 were involved. The complete transient can be well fitted by two single exponential transients with two different time constants. The extracted time constants were 0.21 and 1.40 s for E2 and E3, respectively. Laplace ODLTS was also employed to precisely distinguish individual contributions of adjacent traps, as shown in Fig. 4(b).

Two well-resolved signal peaks, representing electron traps E2 and E3 were obtained in Laplace ODLTS spectra at four fixed temperatures from 290 to 305 K. The magnitude of E3 is much larger than E2, indicating E3 is acting as a dominant trap over E2. Moreover, at elevating temperatures, both E2 and E3 show relatively smaller time constant as indicated by the peak location at different temperature steps. Figure 4(c) shows the extracted temperature-dependent emission time constants from Laplace ODLTS. From 290 to 305 K, the thermally enhanced emission time constants of E2 and E3 were

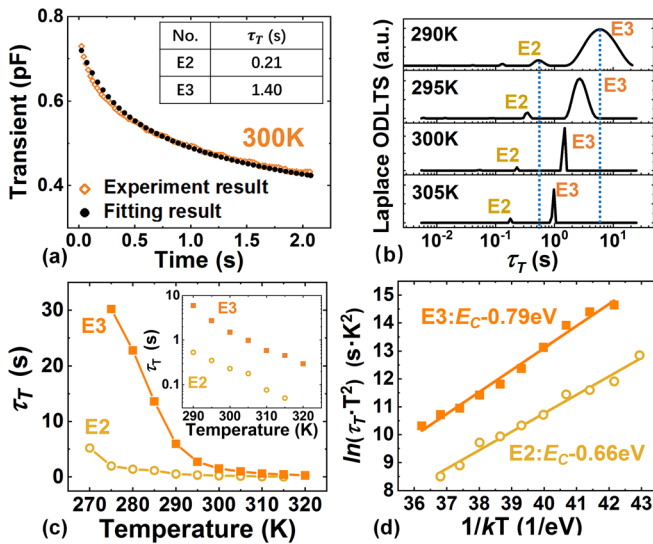


**FIG. 4.** (a) Transient curve fitted with two exponential components at 300 K. (b) Representative Laplace ODLTS spectra from 290 to 305 K. (c) The temperature-dependent  $\tau_T$  of E2 and E3 traps extracted from Laplace ODLTS. Inset:  $\tau_T$  in the logarithm scale as a function of temperature from 290 to 320 K. (d) Arrhenius plots of electron traps E2 and E3 extracted from Laplace ODLTS spectra.

shortened from 0.54 to 0.18 s and from 5.95 to 0.98 s, respectively. Due to the fact that the minority carrier emission process was accelerated as the temperature rises, an insignificant  $V_{th}$  shift and a fast recovery behavior would be expected for *p*-GaN gate HEMTs, justifying its capability of working properly at high temperatures.<sup>35</sup>

Figure 4(d) shows the Arrhenius plot of electron traps E2 and E3 based on the time constants extracted from Laplace ODLTS spectra. The activation energy of E2 and E3 were well resolved and extracted to be  $0.66 \pm 0.02$  and  $0.79 \pm 0.02$  eV, respectively, in good agreement with trap levels extracted from temperature-scanning ODLTS (Fig. 2). Although a deep level similar to E2 has been reported before,<sup>36</sup> its emission time constant is still unknown. Laplace ODLTS managed to reveal the emission time constant of individual traps and their temperature dependence in this study. The trap concentration of E3 ( $N_T = 1.08 \times 10^{15} \text{ cm}^{-3}$ ) is nearly one order of magnitude higher than an electron trap  $E_{p2}$  in *p*-GaN ( $E_C - 0.79 \text{ eV}$ ,  $N_T = 2.30 \times 10^{14} \text{ cm}^{-3}$ ), as reported in the literature.<sup>36</sup> In addition, trap E3 exhibits a larger capture cross section of  $2.57 \times 10^{-13} \text{ cm}^2$ , compared with  $E_{p2}$  in *p*-GaN ( $\sigma_n$  of  $5.9 \times 10^{-14} \text{ cm}^2$ ). The relatively large  $\sigma_n$  suggested that trap E3 is likely complexes or dislocation related.<sup>36</sup> A capture cross section at an order of  $10^{-13} \text{ cm}^2$  has recently been reported for Shockley-Read-Hall (SRH)-type nonradiative recombination centers (NRCs) in Mg-doped GaN, which was believed to be originated from  $V_{Ga}(V_N)_{2-3}$ .<sup>17,37</sup> Based on the trap density and capture cross section, the minority carrier lifetime<sup>17,37</sup> of E3 was calculated to be  $\sim 90$  ps, indicating that the minority carrier capture process could be executed much faster than the corresponding minority carrier emission process.

Figures 5(a)–5(c) illustrate 3D mappings of capacitance transient  $\Delta C(t)$  for traps E1, E2, and E3, respectively. For each measurement, the optical pulse duration ( $t_{po}$ ) was varied to fill the traps to a different extent. When the light injection was switched off, a capacitance transient as a result of the thermal emission of electrons from the filled traps was measured. The black dashed lines of each transient graph represent the projections of transient

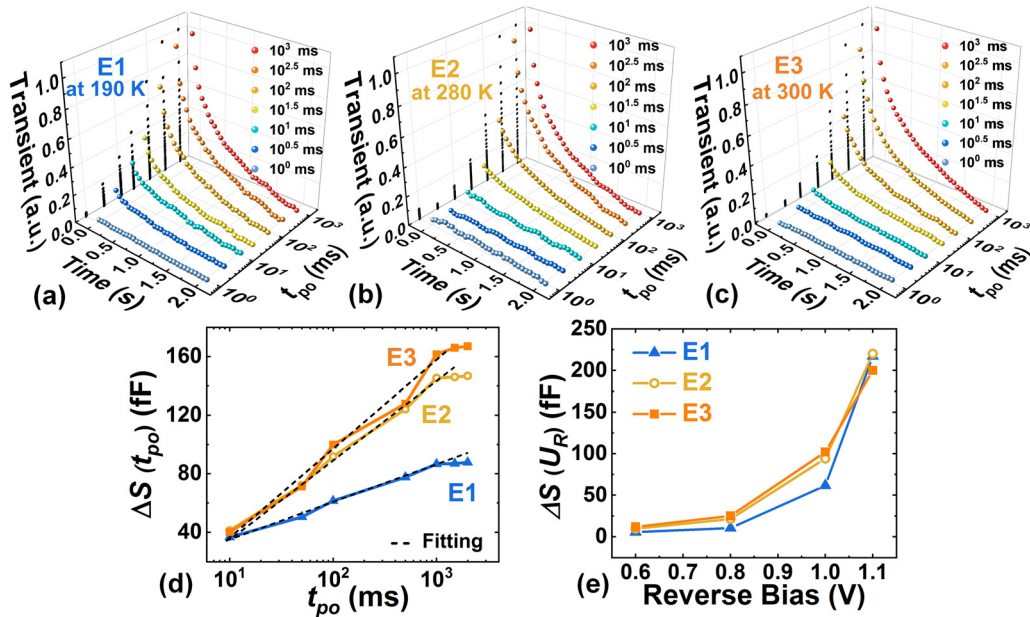


**FIG. 5.** Normalized 3D mapping of ODLTS capacitance transients  $\Delta C(t)$  as a function of the optical pulse duration ( $t_{po}$ ) for (a) E1 (at 190 K), (b) E2 (at 280 K), and (c) E3 (at 300 K) with a fixed  $U_R$  of  $-1 \text{ V}$ . (d) The maximum extent of ODLTS valleys  $\Delta S(t_{po})$  of three electron levels as a function of  $t_{po}$ . (e) Variation of the maximum extent  $\Delta S(U_R)$  in ODLTS spectra of three electron traps as a function of the reverse bias.

amplitudes. A larger optical pulse duration ( $t_{po}$ ) could fill the traps to a higher level, as evidenced by the enhanced intensity of the capacitance transient when extending  $t_{po}$ . For each curve, the cease of  $\Delta C(t)$  with time follows approximately mono-exponential dependence.

As shown in Fig. 5(d), increasing  $t_{po}$  makes the number of injected carriers to be captured as the traps increase,<sup>38,39</sup> and thereby the maximum extent of ODLTS valleys  $\Delta S(t_{po})$  enhances. The amplitude of  $\Delta S(t_{po})$  is nearly saturated until  $t_{po}$  above 1 s. The  $\Delta S(t_{po})$  of E2 and E3 are increasing in a faster rate than E1, which indicates the electron capture kinetics for E2 and E3 are larger than E1. In the graph, the slopes of E2 and E3 are close to each other, indicating that they hold the comparable capability of capturing electrons, as is consistent with the results in Table I.

It should be noted that the amplitude of ODLTS in Figs. 5(d) and 5(e) is proportional to the amplitude of transients in Figs. 5(a)–5(c), but the two values are not necessarily equal to each other. Figure 5(e) shows the ODLTS signal  $\Delta S(U_R)$  as a function of the reverse bias. The amplitude of ODLTS is corresponding to the trap concentration. With low reverse bias ( $U_R < -0.8$  V), the signals of traps were barely observed. The amplitude of ODLTS signals was increased when reverse bias becomes strengthened, indicating that the three electron traps are charged rather than being electrically neutral when being filled. The amplitude dependence on reverse bias also suggested that the traps were not surface related<sup>40</sup> while located inside the *p*-GaN layer.<sup>41,42</sup>

In summary, minority carrier (electron) traps in the *p*-GaN layer of Schottky type *p*-GaN HEMTs were studied by various ODLTS methods. Three electron traps were revealed by temperature-scanning ODLTS. Laplace ODLTS was employed to distinguish two neighboring traps (E2 and E3), which formed a relatively broad signal valley in temperature-scanning ODLTS. Temperature-dependent emission time constants of three trap levels including E1, E2, and E3 were investigated by Laplace ODLTS, showing the emission process was accelerated with increasing temperature. As varying the optical pulse durations, a 3D mapping of the capacitance transient graph was obtained for each deep-level trap. The carrier capture kinetic of three electron traps was studied, indicating all the traps are located inside the *p*-GaN layer rather than surface related. The extraction of minority carrier trap properties in the *p*-GaN layer supplies solid evidence for understanding the dynamic degradation of *p*-GaN gate HEMTs and provides a valuable guideline for further optimization of III-N devices with a *p*-GaN layer.

See the [supplementary material](#) for Laplace ODLTS principles to extract the trap parameters.

This work was supported by the ShanghaiTech University Startup Fund via No. 2017F0203-000-14, the National Natural Science Foundation of China (Grant No. 52131303), the National Science Foundation of Shanghai (Grant No. 22ZR1442300), and in part by the CAS Strategic Science and Technology Program under Grant No. XDA18000000.

## AUTHOR DECLARATIONS

### Conflict of Interest

The authors have no conflicts to disclose.

## DATA AVAILABILITY

The data that support the findings of this study are available from the corresponding author upon reasonable request.

## REFERENCES

- <sup>1</sup>N. Modolo, C. De Santi, A. Minetto, L. Sayadi, S. Sicre, G. Precht, G. Meneghesso, E. Zanoni, and M. Meneghini, *IEEE Electron Device Lett.* **42**(5), 673 (2021).
- <sup>2</sup>N. Chowdhury, J. Lemettinen, Q. Xie, Y. Zhang, N. S. Rajput, P. Xiang, K. Cheng, S. Suihkonen, H. W. Then, and T. Palacios, *IEEE Electron Device Lett.* **40**(7), 1036 (2019).
- <sup>3</sup>Y. T. Gu, Y. Q. Wang, J. X. Chen, B. L. Chen, M. J. Wang, and X. B. Zou, *IEEE Trans. Electron Devices* **68**(7), 3290 (2021).
- <sup>4</sup>J. Wei, G. Tang, R. Xie, and K. J. Chen, *Jpn. J. Appl. Phys., Part 1* **59**(SG), SG0801 (2020).
- <sup>5</sup>L. Sayadi, G. Iannaccone, S. Sicre, O. Haberen, and G. Curatola, *IEEE Trans. Electron Devices* **65**(6), 2454 (2018).
- <sup>6</sup>S. J. Li, Z. Y. He, R. Gao, Y. Q. Chen, Y. Chen, C. Liu, Y. Huang, and G. Q. Li, *IEEE Trans. Electron Devices* **68**(1), 443 (2021).
- <sup>7</sup>Y. Q. Chen, J. T. Feng, J. L. Wang, X. B. Xu, Z. Y. He, G. Y. Li, D. Y. Lei, Y. Chen, and Y. Huang, *IEEE Trans. Electron Devices* **67**(2), 566 (2020).
- <sup>8</sup>X. Chen, Y. Z. Zhong, Y. Zhou, S. Su, S. M. Yan, X. L. Guo, H. W. Gao, X. N. Zhan, S. H. Ouyang, Z. H. Zhang, W. G. Bi, Q. Sun, and H. Yang, *Appl. Phys. Lett.* **119**(6), 063501 (2021).
- <sup>9</sup>R. Wang, J. M. Lei, H. Guo, R. Li, D. J. Chen, H. Lu, R. Zhang, and Y. D. Zheng, *IEEE Electron Device Lett.* **42**(10), 1508 (2021).
- <sup>10</sup>A. N. Tallarico, S. Stoffels, N. Posthuma, P. Magnone, D. Marcon, S. Decoutere, E. Sangiorgi, and C. Fiegna, *IEEE Trans. Electron Devices* **65**(1), 38 (2018).
- <sup>11</sup>T. Katsuno, M. Kanechika, K. Itoh, K. Nishikawa, T. Uesugi, and T. Kachi, *Jpn. J. Appl. Phys., Part 1* **52**(4), 04CF08 (2013).
- <sup>12</sup>T. Narita, K. Tomita, Y. Tokuda, T. Kogiso, M. Horita, and T. Kachi, *J. Appl. Phys.* **124**(21), 215701 (2018).
- <sup>13</sup>T. Narita, Y. Tokuda, T. Kogiso, K. Tomita, and T. Kachi, *J. Appl. Phys.* **123**(16), 161405 (2018).
- <sup>14</sup>H. Y. Huang, X. L. Yang, S. Wu, J. F. Shen, X. G. He, L. Wei, D. S. Liu, F. J. Xu, N. Tang, X. Q. Wang, W. K. Ge, and B. Shen, *Appl. Phys. Lett.* **117**(11), 112103 (2020).
- <sup>15</sup>K. Fu, H. Q. Fu, H. X. Liu, S. R. Alugubelli, T. H. Yang, X. Q. Huang, H. Chen, I. Baranowski, J. Montes, F. A. Ponce, and Y. J. Zhao, *Appl. Phys. Lett.* **113**(23), 233502 (2018).
- <sup>16</sup>S. Yang, S. Huang, J. Wei, Z. Y. Zheng, Y. R. Wang, J. B. He, and K. J. Chen, *IEEE Electron Device Lett.* **41**(5), 685 (2020).
- <sup>17</sup>K. Shima, H. Iguchi, T. Narita, K. Kataoka, K. Kojima, A. Uedono, and S. F. Chichibu, *Appl. Phys. Lett.* **113**(19), 191901 (2018).
- <sup>18</sup>K. Shima, R. Tanaka, S. Takashima, K. Ueno, M. Edo, K. Kojima, A. Uedono, S. Ishibashi, and S. F. Chichibu, *Appl. Phys. Lett.* **119**(18), 182106 (2021).
- <sup>19</sup>G. Miceli and A. Pasquarello, *Phys. Rev. B* **93**(16), 165207 (2016).
- <sup>20</sup>K. Kanegae, H. Fujikura, Y. Otoki, T. Konno, T. Yoshida, M. Horita, T. Kimoto, and J. Suda, *Appl. Phys. Lett.* **115**(1), 012103 (2019).
- <sup>21</sup>Y. Tokuda, *ECS Trans.* **75**(4), 39 (2016).
- <sup>22</sup>K. Kanegae, T. Narita, K. Tomita, T. Kachi, M. Horita, T. Kimoto, and J. Suda, *Appl. Phys. Express* **14**(9), 091004 (2021).
- <sup>23</sup>P. Kruszewski, P. Kaminski, R. Kozlowski, J. Zelazko, R. Czernecki, M. Leszczynski, and A. Turos, *Semicond. Sci. Technol.* **36**(3), 035014 (2021).
- <sup>24</sup>G. Alfieri and T. Kimoto, *Appl. Phys. Lett.* **102**(15), 152108 (2013).
- <sup>25</sup>J. X. Chen, M. Zhu, X. Lu, and X. B. Zou, *Appl. Phys. Lett.* **116**(6), 062102 (2020).
- <sup>26</sup>A. Y. Polyakov and I.-H. Lee, *Mater. Sci. Eng.: R* **94**, 1–56 (2015).
- <sup>27</sup>Y. Tokuda, “Traps in MOCVD n-GaN studied by deep level transient spectroscopy and minority carrier transient spectroscopy,” in *Proceedings of International Conference on Compound Semiconductor Manufacturing Technology (CS MANTECH)*, Denver, Colorado, 19–22 May 2014 (Beaverton, OR, 2014) p. 19.
- <sup>28</sup>M. Meneghini, C. De Santi, I. Abid, M. Buffolo, M. Cioni, R. A. Khadar, L. Nela, N. Zagni, A. Chini, F. Medjdoub, G. Meneghesso, G. Verzellesi, E. Zanoni, and E. Matioli, *J. Appl. Phys.* **130**(18), 181101 (2021).

- <sup>29</sup>A. R. Arehart, A. Corrion, C. Poblentz, J. S. Speck, U. K. Mishra, and S. A. Ringel, *Appl. Phys. Lett.* **93**(11), 112101 (2008).
- <sup>30</sup>G. Alfieri and V. K. Sundaramoorthy, *J. Appl. Phys.* **126**(12), 125301 (2019).
- <sup>31</sup>A. R. Peaker, V. P. Markevich, and J. Coutinho, *J. Appl. Phys.* **123**(16), 161559 (2018).
- <sup>32</sup>C. A. Hernandez-Gutierrez, Y. L. Casallas-Moreno, V. T. Rangel-Kuoppa, D. Cardona, Y. Hu, Y. Kudriatsev, M. A. Zambrano-Serrano, S. Gallardo-Hernandez, and M. Lopez-Lopez, *Sci. Rep.* **10**(1), 16858 (2020).
- <sup>33</sup>Y. Tokuda, Y. Yamada, T. Shibata, S. Yamaguchi, H. Ueda, T. Uesugi, and T. Kachi, *Phys. Status Solidi C* **8**, 2239 (2011).
- <sup>34</sup>P. C. Hsu, E. Simoen, H. Liang, B. De Jaeger, B. Bakeroot, D. Wellekens, and S. Decoutere, *Phys. Status Solidi A* **218**(23), 2100227 (2021).
- <sup>35</sup>J. Chen, M. Hua, J. Wei, J. He, C. Wang, Z. Zheng, and K. J. Chen, *IEEE J. Emerging Sel. Top. Power Electron.* **9**(3), 3686 (2021).
- <sup>36</sup>X. S. Nguyen, X. L. Goh, L. Zhang, Z. Zhang, A. R. Arehart, S. A. Ringel, E. A. Fitzgerald, and S. J. Chua, *Jpn. J. Appl. Phys., Part 1* **55**(6), 060306 (2016).
- <sup>37</sup>S. F. Chichibu, K. Shima, K. Kojima, S. Takashima, M. Edo, K. Ueno, S. Ishibashi, and A. Uedono, *Appl. Phys. Lett.* **112**(21), 211901 (2018).
- <sup>38</sup>J. Criado, A. Gomez, E. Calleja, and E. Muñoz, *Appl. Phys. Lett.* **52**(8), 660 (1988).
- <sup>39</sup>D. Pons, *J. Appl. Phys.* **55**(10), 3644 (1984).
- <sup>40</sup>J. X. Chen, H. X. Luo, H. L. Qu, M. Zhu, H. W. Guo, B. L. Chen, Y. J. Lv, X. Lu, and X. B. Zou, *Semicond. Sci. Technol.* **36**(5), 055015 (2021).
- <sup>41</sup>K. Kanegae, M. Horita, T. Kimoto, and J. Suda, *Appl. Phys. Express* **11**(7), 071002 (2018).
- <sup>42</sup>P. Ferrandis, M. Charles, Y. Baines, J. Buckley, G. Garnier, C. Gillot, and G. Reimbold, *Jpn. J. Appl. Phys., Part 1* **56**(4), 04CG01 (2017).